Quantum transport of atoms in an optical lattice

P. M. Visser and G. Nienhuis
Huygens Laboratorium, Rijksuniversiteit Leiden, Postbus 9504, 2300 RA Leiden, The Netherlands
(Received 4 February 1997)

Quantum-mechanical transport of atoms in an optical lattice in one dimension is described in an exactly solvable model. The atoms are tightly bound and they are sufficiently cooled so that they are restricted only to the lowest Bloch band in a single adiabatic potential. The coherent spreading of an atomic wave packet by tunneling is counteracted by the localizing effect of photon emission that accompanies optical pumping. The time evolution of the quasimomentum distribution, the coherence length, and the spatial width of the atomic state are evaluated analytically. These quantities depend strongly on the statistics of photon emissions. [S1050-2947(97)01811-8]

PACS number(s): 42.50.Vk, 32.80.Pj, 05.60.+w

I. INTRODUCTION

A monochromatic radiation field, composed of a few plane traveling waves, may present a periodic potential to atoms as a result of spatially varying light shifts. In the past few years, it has become feasible to trap atoms in the potentials wells and to form an optical lattice [1–6]. The long-range order of this lattice is imposed by the radiation field and it does not depend on the interatomic interactions. Moreover, the filling factor of the lattice sites is usually low. In such a situation, the transport properties of atoms in an optical lattice are governed entirely by the atom-field interaction. Recently, the loss rate by spontaneous emission of Li atoms trapped in an optical lattice has been measured [7]. The successive escape of a Rb atom from a well and its recapture by a neighboring one have been investigated by observing polarization-dependent intensity correlations of the emitted fluorescence [8]. Other recent work of dynamics of atoms in periodic optical potentials include the observation of Bloch oscillations [9] and the observation of atomic Wannier-Stark ladders [10,11].

When an atom is deeply cooled, the wave nature of its translational degree of freedom must be accounted for and the wave function can be expected to extend over various lattice sites. The time-dependent evolution of an atomic wave packet under the combined influence of the periodic potential and spontaneous emission can be viewed as a prototypical case of quantum transport. In a recent paper [12], Marksteiner *et al.* study the anomalous diffusion of two-level atoms in optical molasses by the quantum Monte Carlo method. This anomalous diffusion, which can be pictured as a Lévy walk in space, occurs when atoms get excited to above the potential barrier.

In the present paper we consider a model system that is sufficiently simple to be treated analytically and contains, nonetheless, essential ingredients of experimental situations. The lattice is modeled as a periodic adiabatic potential in one dimension. We assume that cooling is sufficiently effective so that only the lowest-energy band in the potential is occupied. We evaluate the time evolution of the translational state in the tight-binding limit, where the lowest state of the atom in one potential well is only coupled to its nearest neighbors. The adiabatic internal state of the atom has a position-dependent admixture of the excited state, which gives rise to spontaneous emission. In the presence of sufficiently strong cooling, this may be viewed as optical pumping within the lowest-energy band. The coherent process of tunneling between neighboring wells, which generally increases the coherence length, and the dissipative process of optical pumping, which tends to localize the atom, are the main ingredients of the transport process. We apply the model in a trajectory description of the atomic motion, where optical pumping is represented as a quantum jump interrupting the coherent evolution between jumps. We compare two complementary but equivalent pictures of optical pumping. In one, the momenta of the emitted photons are measured, which results in a Brownian motion of the atomic momentum. In the other picture, the positions are measured from where the photons originate, which has the effect of localizing the atom in a single well. The jump-free evolution allows atoms to tunnel from one well to the next.

We also study the situation that a dark state is present in the energy band. This case is modeled by setting the decay rate at the bottom edge of the band equal to zero. For a nearby Bloch state, the average waiting time between two jumps becomes infinite and the jumps are governed by Lévy statistics [13].

II. BLOCH AND WANNIER STATES IN A PERIODIC POTENTIAL

A. General transformation properties

The translational motion of atoms in a spatially periodic light field with variation in one dimension is described by the effective Hamiltonian

$$\boldsymbol{H}=\frac{\boldsymbol{P}^2}{2m}+V(\boldsymbol{x}),$$

with $V(x)$ a real periodic potential with period a. The energy eigenstates can be chosen to be also eigenstates of the displacement operator $\boldsymbol{T}$, which translates a wave function over a, according to the relation

$$\boldsymbol{T}|x\rangle=|x+a\rangle.$$

The combined eigenstates of $\boldsymbol{H}$ and $\boldsymbol{T}$ have energy eigenvalues $E_j(p)$ that separate in a discrete set of energy bands. The energy eigenvalue equation is then

$$\boldsymbol{H}|E_j(p)\rangle = E_j(p)|E_j(p)\rangle. \tag{2.1}$$

For each value of the discrete index j, the energy is a function of the Bloch index p, which is determined by the unitary eigenvalue of $\boldsymbol{T}$, according to the relation [14]

$$\boldsymbol{T}|E_j(p)\rangle = e^{-2\pi i p}|E_j(p)\rangle. \tag{2.2}$$

We shall assume that sub-Doppler cooling is sufficiently strong so that only the first energy band is populated appreciably. While this assumption may seem rather optimistic compared to present-day experiments, it is not fully unrealistic, and progress in this direction is substantial [15–18]. Then we consider only this lowest band and we suppress the band index j. We can restrict p to the first Brioullin zone $[-\frac{1}{2},\frac{1}{2}]$. The quasimomentum of a state with Bloch index p is equal to bp, with $b=2\pi/a$ the reciprocal lattice constant. Since the Hamiltonian is real in coordinate representation, it obeys time-reversal invariance, so that the energy $E(p)$ is an even function of p.

The Bloch condition (2.2) defines p only mod1, so that the eigenstates $E(p)$ and eigenvectors $|E(p)\rangle$ are periodic functions of the Bloch index p with period 1. Therefore, they can be expanded as Fourier series. This gives for the energy band

$$E(p)=\sum_n e^{2\pi i n p}E_n, \tag{2.3}$$

with real coefficients $E_n=E_{-n}$. For the Bloch states we find

$$|E(p)\rangle=\sum_n e^{2\pi i n p}|\phi_n\rangle. \tag{2.4}$$

The coefficients $|\phi_n\rangle$ form a discrete set of states, called Wannier states [14]. The inverse relation of Eq. (2.4) is

$$|\phi_n\rangle=\int dp e^{-2\pi i n p}|E(p)\rangle. \tag{2.5}$$

The integration over p extends over the Brillouin zone in this and all subsequent integrals.

Since the Bloch states are spatially unbounded, they must be normalized to a δ function, and we take

$$\langle E(p')|E(p)\rangle=\delta(p'-p). \tag{2.6}$$

From the orthonormality relation (2.6) of the Bloch states one shows that

$$\langle\phi_{n'}|\phi_n\rangle=\delta_{n'n}, \tag{2.7}$$

so that the Wannier states are also orthonormal. This implies that they have a finite spatial extent. Substitution of Bloch's theorem (2.2) into Eq. (2.5) shows that

$$\boldsymbol{T}|\phi_n\rangle=|\phi_{n+1}\rangle,$$

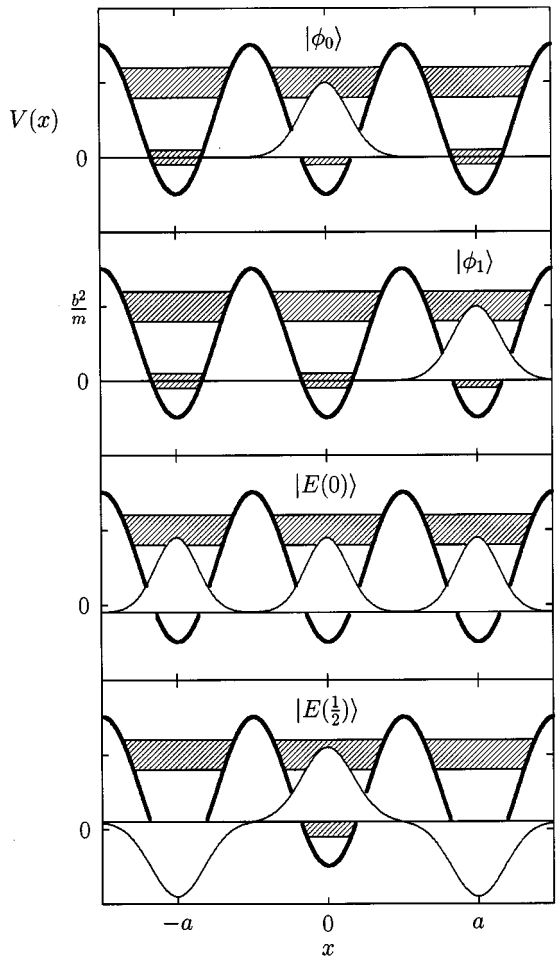

FIG. 1. Sketch of energy bands and Wannier and Bloch wave functions in a cosine potential $V(x)$. The barrier height is chosen as $2b^2/m$. The Wannier wave functions $|\phi_n\rangle$ are localized around the potential minima $x_n=na$, as demonstrated in the top two figures for $n=0$ and 1. The Bloch states $|E(0)\rangle$ and $|E(\frac{1}{2})\rangle$ lie at the bottom and top of the first energy band. Their real wave functions are extended over all the wells as indicated in the bottom two plots.

so that $|\phi_n\rangle$ is related by $|\phi_0\rangle$ by a translation over na. The properties of Bloch and Wannier states are illustrated in Fig. 1.

Since the Wannier states form an orthonormal basis of states in the energy band, one may conclude that the single state $|\phi_0\rangle$ completely defines all states in the energy band. This statement is illustrated by expanding the Bloch state in plane waves $|k\rangle$. It is obvious from Eq. (2.2) that $|E(p)\rangle$ contains only the discrete set of plane-wave components $|(n+p)b\rangle$. To be specific, when the plane-wave states are normalized as $\langle k'|k\rangle=\delta(k'-k)$, we find from Eq. (2.4) the equality

$$|E(p)\rangle=b\sum_n |(n+p)b\rangle\langle(n+p)b|\phi_0\rangle.$$

If we substitute the expansion (2.4) in the eigenvalue relation (2.1) and take the inner product with the Wannier state $\langle\phi_{n'}|$, we find with the orthonormality relation (2.7) that

$$\langle\phi_{n'}|\boldsymbol{H}|\phi_n\rangle=E_{n-n'}.$$

Hence the Fourier coefficients E_n of the energy coincide with the matrix elements of the Hamiltonian between Wannier states.

B. Tight-binding model

The relations between the Bloch and Wannier states as discussed so far are exact. We want to consider in particular the situation that the atoms are tightly bound near the bottom of the potential wells, which can be assumed to be located at the positions $x_n = na$. This tight-binding assumption is justified when the depth of the potential wells is large compared to the minimal kinetic energy of a particle localized in a well, which is of the order of $b^2/2m$ ($\hbar = 1$). Then we may assume that the Wannier state $|\phi_n\rangle$ is mainly located within a single well, which we can take to be the well at x_n. This implies that the Fourier coefficients E_n fall off with increasing values of n, and we take only the coupling between neighboring wells into account. The dispersion relation (2.3) is then parametrized as

$$E(p) = -E\ \cos 2\pi p, \tag{2.8}$$

with $E = -2E_1 > 0$. The energy band extends from the ground state $|E(0)\rangle$, with Bloch index $p = 0$ and energy $-E$, to the state $|E(\frac{1}{2})\rangle$, which is located at energy E at the top of the band edge. These states are sketched in Fig. 1, along with the Wannier states $|\phi_0\rangle$ and $|\phi_1\rangle$.

When spontaneous emission is neglected and the total evolution is governed by the Hamiltonian, the spreading of an initially localized state in this tight-binding limit is very simple. When the initial state $|\psi(0)\rangle = |\phi_0\rangle$ is localized in well 0, the time-dependent state is immediately found after using the expansion (2.5) in Bloch states and using the energy eigenvalue relation (2.1). After using the defining relation of the Bessel functions J_n, which follows from Eq. (A2) after substituting $\Gamma_1 = iE$ while using $I_n(\Gamma_1 t) = i^n J_n(Et)$, we obtain the time-dependent state

$$|\psi(t)\rangle = \sum_n\ i^n J_n(Et)|\phi_n\rangle. \tag{2.9}$$

This result describes the time-dependent spreading of an initially localized state over the wells by tunneling through the barriers. The resulting distribution over the wells has an analytic behavior very similar to the distribution over transverse momentum of atoms diffracted by a standing wave [19].

III. SPONTANEOUS DECAY

As noted above, the present model is based on the assumption that an atom is at all times in the internal state corresponding to an adiabatic periodic potential and that it resides in the lowest-energy band in this potential. Due to the small excited-state amplitudes in the adiabatic internal state, the atom has a finite probability of spontaneous emission. In the presence of a sub-Doppler cooling mechanism we can assume that this emission process corresponds to optical pumping within the lowest-energy band. Typical for situations of sub-Doppler cooling is that the rate of optical pumping depends on both position and velocity. For example, Sisyphus cooling requires that the optical pumping rate is higher at positions with a high optical potential, which leads to a highly sensitive dependence of the net force on the velocity. Then Bloch states that are better localized near the potential minima can be expected to have smaller decay rates. This justifies the assumption that the rate of optical pumping $\Gamma(p)$ of the Bloch state $|E(p)\rangle$ will depend on the index p. In the tight-binding limit, it is reasonable to assume that the decay operator couples only nearest-neighbor Wannier states. In analogy to Eq. (2.8), this leads to the parametrization

$$\Gamma(p) = \Gamma_0 - \Gamma_1 \cos 2\pi p \tag{3.1}$$

for the optical pumping rate.

Interesting effects can arise when the atom is pumped into a dark state. This is the case when the carrier waves of the optical lattice drive a transition between levels with angular momenta $J \to J-1$ and $J \to J$ for integer J values. In this case an effective periodic potential can still arise due to a magnetic field [5] or due to nonadiabatic interactions [20]. We will also consider the case of the presence of an exact black state to study velocity-selective coherent population trapping (VSCPT). We model this situation by taking $\Gamma(0) = 0$. The resulting tight-binding form (3.1) with $\Gamma_0 = \Gamma_1$ is realized in the periodic gauge potential of the VSCPT system [20]. In this case, also the form (2.8) for the energy holds.

The dynamics in the fundamental energy band is governed by the master equation for the reduced density operator $\boldsymbol{\rho}$ for the first energy band alone:

$$\frac{d}{dt}\,\boldsymbol{\rho}(t) = i[\boldsymbol{\rho}(t), \boldsymbol{H}] - \tfrac{1}{2}[\boldsymbol{\Gamma}\boldsymbol{\rho}(t) + \boldsymbol{\rho}(t)\boldsymbol{\Gamma}] + \mathcal{G}\boldsymbol{\rho}(t), \tag{3.2}$$

where $\boldsymbol{\Gamma}$ is an optical pumping operator. On the basis of Bloch states, the Hamiltonian and the optical pumping operators are diagonal, so that

$$\boldsymbol{H}|E(p)\rangle = E(p)|E(p)\rangle, \quad \boldsymbol{\Gamma}|E(p)\rangle = \Gamma(p)|E(p)\rangle,$$

where the energy $E(p)$ is given by Eq. (2.8) and the decay rate $\Gamma(p)$ by Eq. (3.1). The (super)operator $\mathcal{G}$, which acts on density matrices, describes the gain that results from the optical pumping process. Its action is the multiplication of the atomic wave function with the mode function of the optical mode from which the atom absorbs a photon and the complex conjugate of the mode function in which the atom emits. The net result of the optical pumping cycle is a momentum recoil of the atom, which we model by a shift of the wave function in quasimomentum space by q. In the spirit of our assumption that the atomic state remains in the lowest-energy band, this effect is modeled by changing the state $|E(p)\rangle$ into the state $|E(p-q)\rangle$. When we assume for simplicity that the distribution over the momentum recoil q is uniform over the Brillouin zone, both the loss and the gain term in the master equation (3.2) can be expressed in the q-dependent operator $\boldsymbol{A}(q)$ defined by

$$\boldsymbol{A}(q)|E(p)\rangle = |E(p-q)\rangle\sqrt{\Gamma(p)}. \tag{3.3}$$

We may write

$$\mathcal{G}\boldsymbol{\rho}=\int dq\boldsymbol{A}(q)\boldsymbol{\rho}\mathbf{A}^{\dagger}(q),\quad \boldsymbol{\Gamma}=\int dq\boldsymbol{A}^{\dagger}(q)\boldsymbol{A}(q). \tag{3.4}$$

After substitution of Eq. (3.4), the master equation (3.2) has its standard Lindblad form, where the operators $\boldsymbol{A}(q)$ serve as the jump operators [21]. The total photon emission rate

$$f(t)=\mathrm{tr}\mathcal{G}\boldsymbol{\rho}(t)=\mathrm{tr}\boldsymbol{\Gamma}\boldsymbol{\rho}(t) \tag{3.5}$$

is the integral over the partial rate with recoil q,

$$f(q,t)=\mathrm{tr}\boldsymbol{A}(q)\boldsymbol{\rho}(t)\boldsymbol{A}^{\dagger}(q).$$

The decomposition of the master equation in jump operators is not unique and the general form remains invariant under an arbitrary unitary transformation [22–24]. A complementary expansion of the gain and loss terms is obtained by the unitary transformation

$$\boldsymbol{A}_n=\int dqe^{2\pi inq}\boldsymbol{A}(q). \tag{3.6}$$

The gain operator and the optical pumping operator (3.4) can alternatively be expressed in terms of the jump operators $\boldsymbol{A}_n$, with the result

$$\mathcal{G}\boldsymbol{\rho}=\sum_n \boldsymbol{A}_n\boldsymbol{\rho}\mathbf{A}_n^{\dagger},\quad \boldsymbol{\Gamma}=\sum_n \boldsymbol{A}_n^{\dagger}\boldsymbol{A}_n. \tag{3.7}$$

The operator $\boldsymbol{A}_n$ represents optical pumping, where the emitted photon is detected near the well at $x_n=na$. As a result of this detection, the atom is localized in the Wannier state $|\phi_n\rangle$. This can be seen by expressing the operator in terms of the Wannier states. After substituting Eq. (2.4) in the right-hand side of Eq. (3.3), one finds from Eq. (3.6)

$$\boldsymbol{A}_n|\phi_{n'}\rangle=|\phi_n\rangle\int dp\sqrt{\Gamma(p)}e^{2\pi i(n-n')p}.$$

For a uniform decay rate $\Gamma(p)=\Gamma_0$, the operator $\boldsymbol{A}_n$ is equal to $\sqrt{\Gamma_0}$ times the projector on the Wannier state $|\phi_n\rangle$. In this case, optical pumping does not lead to diffusion of the atom (see Sec. VI B).

The detection rate of photons that localize the atom in $|\phi_n\rangle$ is

$$f_n(t)=\mathrm{tr}\boldsymbol{A}_n\boldsymbol{\rho}(t)\boldsymbol{A}_n^{\dagger}, \tag{3.8}$$

which adds up to the total detection rate (3.5), as

$$f(t)=\int dqf(q,t)=\sum_n f_n(t).$$

When the jump rate Γ is independent of p, the operator $\boldsymbol{A}_n$ is simply a projector on the Wannier state $|\phi_n\rangle$. In this case a localized photon detection is just equivalent to the detection of the atom in the corresponding Wannier state. Due to the p dependence of Γ, also the population of neighboring states contributes to the photon detection rate $f_n(t)$. When the distribution over the values of the recoil q is not uniform over the Brillouin zone, the jump rate Γ in Eq. (3.3) will be a function of both p and q. In that case, the operator $\boldsymbol{A}_n$ will not localize the atom exactly in the Wannier state $|\phi_n\rangle$, but in a linear superposition of neighboring states.

The two sets of jump operators $\boldsymbol{A}(q)$ and $\boldsymbol{A}_n$, as given by Eqs. (3.3) and (3.6), may be viewed as corresponding to detection of a photon with a well-determined momentum bq or a photon at a well-determined location n. This may be identified by a detection in the far or the near field. The relation between $\boldsymbol{A}(q)$ and $\boldsymbol{A}_n$ generalizes a similar distinction between two detection schemes as discussed by Holland *et al.* [25] for free atoms.

IV. TRAJECTORIES

The master equation (3.2) is equivalent to the integral equation of the Dyson type

$$\boldsymbol{\rho}(t)=\boldsymbol{\rho}_0(t)+\int_0^t dt'\mathcal{U}(t-t')\mathcal{G}\boldsymbol{\rho}(t'), \tag{4.1}$$

where the first term

$$\boldsymbol{\rho}_0(t)=\mathcal{U}(t)\boldsymbol{\rho}(0) \tag{4.2}$$

represents the contribution to the density matrix from the situation of zero jumps in the time interval $[0,t]$ in terms of the linear evolution operator $\mathcal{U}(t)$, defined by

$$\mathcal{U}(t)\boldsymbol{\rho}=e^{-i\boldsymbol{H}t-\boldsymbol{\Gamma}t/2}\boldsymbol{\rho}e^{+i\boldsymbol{H}t-\boldsymbol{\Gamma}t/2}.$$

The norm of the operator $p_0(t)=\mathrm{tr}\boldsymbol{\rho}_0(t)$ is the zero-jump probability. The iterated solution of the Dyson equation (4.1) represents the density matrix directly as a weighted average over pure states [26]. In this way the concept of quantum trajectories as pure-state realizations of the evolution of the system is recovered [22,24,27]. Each trajectory consists of a continuous evolution during finite time intervals, which are separated by quantum jumps at random instants of time. For an initially pure state $\boldsymbol{\rho}_0(0)=|\psi(0)\rangle\langle\psi(0)|$, the time-dependent normalized pure-state density matrix up to the instant of the first jump is

$$\boldsymbol{\rho}'(t)=|\psi(t)\rangle\langle\psi(t)|, \tag{4.3}$$

where the state vector can be chosen as

$$|\psi(t)\rangle=\frac{1}{\sqrt{p_0(t)}}e^{-i\boldsymbol{H}t-\boldsymbol{\Gamma}t/2}|\psi(0)\rangle.$$

The time dependence of $|\psi(t)\rangle$ is governed by a nonlinear evolution equation [26]. The instant of the first jump is stochastically determined by the waiting-time distribution

$$w(t)=-\frac{d}{dt}p_0(t)=\mathrm{tr}\mathcal{G}\boldsymbol{\rho}_0(t)=\mathrm{tr}\boldsymbol{\Gamma}\boldsymbol{\rho}_0(t), \tag{4.4}$$

which is the *a priori* probability density that the first jump occurs at time t. A quantity of physical interest is the jump rate at time t under the condition that no jump has occurred in the interval $[0,t]$. This conditional photon emission rate is denoted as

$$f'(t)=\mathrm{tr}\mathcal{G}\boldsymbol{\rho}'(t)=\frac{w(t)}{p_0(t)}.$$

In this and following equations, the prime indicates the no-jump condition. When the gain and loss operators are expressed as an integral over q, or as a summation over n as in Eq. (3.4) or (3.7), the waiting-time distribution $w(t)$ is separated into partial waiting-time distributions $w_n(t)$ or $w(q,t)$. With the form (3.3) of the jump operator $\boldsymbol{A}(q)$, it is easy to check that

$$w(q,t)=\mathrm{tr}\boldsymbol{A}(q)\boldsymbol{\rho}_0(t)\boldsymbol{A}^\dagger(q)=w(t),$$

so that the partial waiting-time distribution $w(q,t)$ is always uniform over the recoil. The conditional rates are likewise separated into partial contributions $f'_n(t)$ or $f'(q,t)$. Note that $p_0(t)$, $w(t)$, $f'(t)$, as well as the partial distributions and rates depend in general on the initial state at the beginning of the time interval.

A realization of a trajectory is generated by drawing a series of random numbers ε_i from the interval [0,1]. After a jump, at the beginning of each jump-free interval at time t_i, the length of the jump-free interval $t=t_{i+1}-t_i$ to the next jump at time t_{i+1} can be determined from $p_0(t)=\varepsilon_i$. In this way the jump times are distributed according to the waiting-time distribution $w(t)$. At each jump instant, the value of the recoil q or the location n of the emitted photon has to be determined by drawing another random number, according to the relative probabilities of these values. The jumps are then described by applying the jump operators $\boldsymbol{A}(q)$ or $\boldsymbol{A}_n$. The resulting quantum trajectories are quite different, depending on which one of the two photon detection schemes is chosen for representing the gain term in the master equation. Trajectories corresponding to a localized photon detection have also been applied to evaluate anomalous diffusion in optical lattices [12].

A. Localization picture

When a photon is detected at time t at the location n, the atom is localized in the Wannier state $|\phi_n\rangle$, as expressed by the jump operator

$$|\psi(t)\rangle\rightarrow\frac{1}{\sqrt{f'_n(t)}}\boldsymbol{A}_n|\psi(t)\rangle=|\phi_n\rangle. \tag{4.5}$$

For an initial Wannier state $|\psi(0)\rangle=|\phi_0\rangle$ at time zero, the zero-jump probability is given by

$$p_0(t)=\int dp e^{-\Gamma(p)t}=e^{-\Gamma_0 t}I_0(\Gamma_1 t), \tag{4.6}$$

where I_n are the modified Bessel functions. The last equality follows from the particular form (3.1) of the decay rate $\Gamma(p)$. For the waiting-time distribution we find with Eq. (4.4)

$$w(t)=e^{-\Gamma_0 t}[\Gamma_0 I_0(\Gamma_1 t)-\Gamma_1 I_1(\Gamma_1 t)],$$

which is the sum over the partial distributions for the next detection of a photon at location n,

$$w_n(t)=\mathrm{tr}\boldsymbol{A}_n\boldsymbol{\rho}_0(t)\boldsymbol{A}_n^\dagger=\left|\int dp e^{-iE(p)t-\Gamma(p)t/2}\sqrt{\Gamma(p)}e^{2\pi inp}\right|^2. \tag{4.7}$$

Naturally, this depends only on the difference in location n. The total conditional emission rate is then

$$f'(t)=\Gamma_0-\Gamma_1\frac{I_1(\Gamma_1 t)}{I_0(\Gamma_1 t)}, \tag{4.8}$$

which is the sum of the conditional partial emission rates

$$f'_n(t)=\mathrm{tr}\boldsymbol{A}_n\boldsymbol{\rho}'(t)\boldsymbol{A}_n^\dagger=\langle\psi(t)|\boldsymbol{A}_n^\dagger\boldsymbol{A}_n|\psi(t)\rangle=\frac{w_n(t)}{p_0(t)}.$$

These partial emission rates as a function of time reflect the spreading of an initially localized atomic state during a jump-free time interval.

A trajectory is thus completely determined by the series of events at times $t_1,t_2,\ldots$, where the atom is detected at well $n_1,n_1+n_2,\ldots$. Immediately after the jump at time t_i, the atom is localized in a Wannier state.

B. Recoil picture

Detection at time t of a photon with momentum bq gives a recoil on the atomic state, as expressed by the jump operator

$$|\psi(t)\rangle\rightarrow\frac{1}{\sqrt{f'(q,t)}}\boldsymbol{A}(q)|\psi(t)\rangle.$$

When the initial state at time zero is the Bloch state $|E(p)\rangle$, the state is unchanged until the first jump. The zero-jump probability is then

$$p_0(t)=e^{-\Gamma(p)t}$$

and the partial waiting-time distribution is

$$w(q,t)=w(t)=\Gamma(p)e^{-\Gamma(p)t}.$$

This implies that the conditional jump rate

$$f'(q,t)=f'(t)=\Gamma(p)$$

is constant in time and uniform in the recoil. These quantities give the statistics of the jump instants $t_1,t_2,\ldots$ and the values of the recoils $q_1,q_2,\ldots$, which completely determine the trajectories in the recoil picture. In this picture, the atom is in a Bloch state at all times. Although the distribution over the quasimomentum shift q is uniform, the statistics of the waiting times depends on the index p_i, which is different for each jump-free time interval. A Bloch state has an infinite coherence length and a homogeneous spatial distribution. Therefore, a single trajectory in the recoil picture does not give information on the evolution of spatial distribution or spatial coherence. On the other hand, the ensemble average of the trajectories in each picture coincides with the solution of the master equation and therefore contains complete information.

V. MOMENTUM DISTRIBUTION AND COHERENCE LENGTH

A. General expressions

The localization picture of trajectories can be conveniently applied to discuss the evolution of the spatial coherence properties of an atom, as described by the solution of the full master equation (3.2). For a given density matrix $\boldsymbol{\rho}(t)$, we introduce the distribution over the Bloch states

$$\rho(p,t)=\langle E(p)|\boldsymbol{\rho}(t)|E(p)\rangle. \tag{5.1}$$

The spatial coherence is characterized by the functions

$$R_m(t)=\sum_n \langle \phi_n|\boldsymbol{\rho}(t)|\phi_{n+m}\rangle=\int dp e^{-2\pi imp}\rho(p,t), \tag{5.2}$$

which are the Fourier coefficients of the quasimomentum distribution (5.1). This shows that a narrow quasimomentum distribution corresponds to a wide characteristic width of R_m as a function of m, which reflects a large coherence length.

We consider the solution of the master equation with Wannier state $|\phi_0\rangle$ as the initial state. Hence the initial momentum distribution is uniform, according to Eq. (2.4). In this case, we wish to evaluate the momentum distribution $\rho(p,t)$ and the total emission rate $f(t)$. First, we notice that the time-dependent zero-jump momentum distribution corresponding to the zero-jump density matrix (4.2) is

$$\rho_0(p,t)=\langle E(p)|\boldsymbol{\rho}_0(t)|E(p)\rangle=e^{-\Gamma(p)t}. \tag{5.3}$$

When we take the diagonal elements of the Dyson equation (4.1) for a Bloch state, while using Eq. (3.5), we obtain the equation

$$\rho(p,t)=\rho_0(p,t)+\int_0^t dt'\rho_0(p,t-t')f(t'). \tag{5.4}$$

We used that in the form (3.7) of the gain operator $\mathcal{G}$, each summand projects the atom in a Wannier state $|\phi_n\rangle$, with a uniform momentum distribution immediately after the jump. As we have shown before [28], a relation similar to Eq. (5.4) holds for the density matrix in the case of a master equation when the gain term puts the system in a unique target state. In the present case, the momentum distribution following a jump is always the same, at least when the jumps are represented in the localization picture. Equation (5.4) expresses the momentum distribution $\rho(p)$ in the zero-jump distribution $\rho_0(p)$ and the jump rate f. In its turn, the jump rate is determined by the waiting-time distribution w. Substitution of Eq. (5.4) into Eq. (3.5) while using Eq. (4.4) leads to the integral equation for the jump rate

$$f(t)=w(t)+\int_0^t dt' w(t-t')f(t').$$

B. Jump rate, momentum distribution, and coherence length

For the Laplace transforms of these quantities, defined in the Appendix, we obtain the standard relations [28–30]

$$1+\hat{f}(\nu)=\frac{1}{1-\hat{w}(\nu)}=\frac{1}{\nu\hat{p}_0(\nu)}, \tag{5.5}$$

which expresses the f to p_0 in the Laplace domain. The momentum distribution $\rho(p)$ in Laplace transform is found from Eq. (5.4) as

$$\hat{\rho}(p,\nu)=\hat{\rho}_0(p,\nu)[1+\hat{f}(\nu)]=\frac{\hat{\rho}_0(p,\nu)}{\nu\hat{p}_0(\nu)}.$$

Use of Eq. (A3) in the Appendix for $m=0$ gives the Laplace transform of the zero-jump probability (4.6) in the form

$$\hat{p}_0(\nu)=\frac{1}{\sqrt{(\nu+\Gamma_0)^2-\Gamma_1^2}}=\frac{1}{\Gamma_1\sinh\beta(\nu)},$$

where the parameter β is defined as $\cosh\beta(\nu)=(\nu+\Gamma_0)/\Gamma_1$. Then Eq. (5.5) gives the Laplace transform of the jump rate

$$\hat{f}(\nu)=\frac{\Gamma_0-\Gamma_1 e^{-\beta(\nu)}}{\nu}, \tag{5.6}$$

and by using Eq. (5.3), we obtain for the Laplace-transformed momentum distribution

$$\hat{\rho}(p,\nu)=\frac{1}{\nu}\frac{\sinh\beta(\nu)}{\cosh\beta(\nu)-\cos2\pi p}.$$

According to Eq. (5.2), the coefficients in the expansion (A1) are precisely the Laplace transforms of the coherence functions R_m, so that we find

$$\hat{R}_m(\nu)=\frac{e^{-|m|\beta(\nu)}}{\nu}. \tag{5.7}$$

By using Eq. (A4) for $m=1$ one obtains an explicit integral expression for the jump rate f, by Laplace inversion of Eq. (5.6), with the result

$$f(t)=\Gamma_0-\Gamma_1\int_0^t dt'\frac{e^{-\Gamma_0 t'}}{t'}I_1(\Gamma_1 t'). \tag{5.8}$$

Substitution of Eq. (5.8) into Eq. (5.4) gives the corresponding integral expression for the momentum distribution

$$\rho(p,t)=e^{-\Gamma(p)t}+\Gamma_0\frac{1-e^{-\Gamma(p)t}}{\Gamma(p)} -\Gamma_1\int_0^t dt'\frac{e^{-\Gamma_0 t'}}{t'}\frac{1-e^{-\Gamma(p)(t-t')}}{\Gamma(p)}I_1(\Gamma_1 t'). \tag{5.9}$$

Integral expressions for the coherence functions $R_m(t)$ follow directly after Laplace inversion of Eq. (5.7), by application of Eq. (A4). The result is

$$R_m(t)=|m|\int_0^t dt'\frac{e^{-\Gamma_0 t'}}{t'}I_m(\Gamma_1 t') \quad \text{if} \quad m\neq 0. \tag{5.10}$$

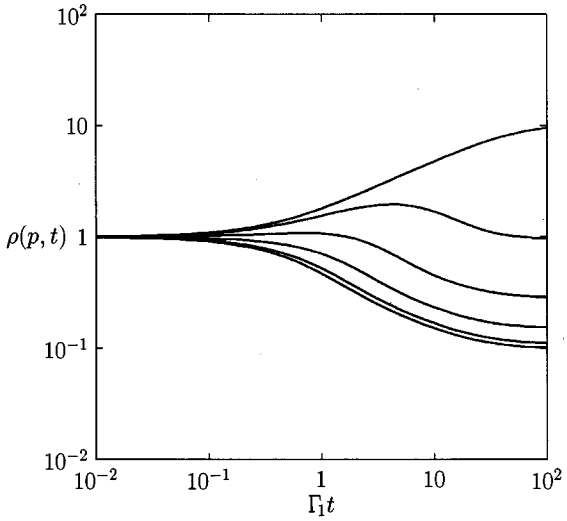

FIG. 2. Quasimomentum distribution $\rho(p,t)$ plotted as a function of time on a double logarithmic scale for $p=0$ to $p=\frac{1}{2}$ with steps $\frac{1}{10}$. Parameters Γ_0,Γ_1 are such that $\Gamma(\frac{1}{2})=100\Gamma(0)$.

Note that the coherence functions are non-negative at all times. These expressions (5.8)–(5.10) can be directly evaluated numerically. Some results are plotted in Figs. 2 and 3. The integrals in Eqs. (5.8)–(5.10) vanish when $\Gamma_1=0$, so that $\Gamma(p)=\Gamma_0$ is uniform over the Brillouin zone. Then $f=\Gamma_0$, $\rho(p)=1$, and $R_m=0$ at all times.

The steady-state values of f, $\rho(p)$, and R_m are found by multiplying their Laplace transforms with ν and taking the limit $\nu\searrow 0$, with the result

$$\overline{f}=\sqrt{\Gamma_0^2-\Gamma_1^2},\quad \overline{\rho(p)}=\frac{\overline{f}}{\Gamma(p)},\quad \overline{R_m}=\left(\frac{\Gamma_0-\overline{f}}{\Gamma_1}\right)^{|m|}.$$

Since the lattice sites are fully equivalent, the steady-state density operator $\overline{\boldsymbol{\rho}}$ is translationaly invariant, so that it is diagonal in Bloch states. Hence $\overline{\boldsymbol{\rho}}$ is fully determined by the steady-state quasimomentum distribution $\overline{\rho(p)}$.

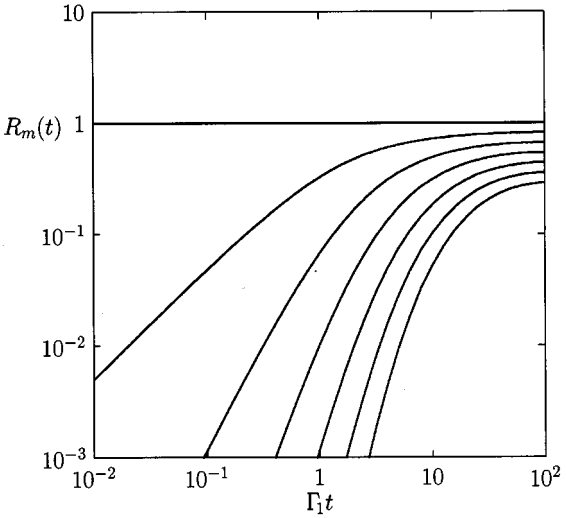

FIG. 3. Spatial coherence functions $R_m(t)$ as a function of time, for $m=0$ (top curve) to $m=6$ (bottom curve), with the same parameters as in Fig. 2.

The asymptotic behavior of f for $t\to\infty$ is found from Eq. (5.6) by applying Eq. (A5) in the case $n=1$ and $\gamma=\Gamma(0)=\Gamma_0-\Gamma_1$. The result is

$$f(t)-\overline{f}\approx\frac{e^{-\Gamma(0)t}}{\Gamma(0)}\sqrt{\frac{\Gamma_1}{2\pi t^3}}.$$

The asymptotic behavior of the momentum distribution is found in the same fashion, with the result

$$\rho(p,t)-\overline{\rho(p)}\approx\frac{f(t)-\overline{f}}{\Gamma(p)-\Gamma(0)}\quad\text{if}\quad p\neq 0,$$

$$\rho(0,t)-\overline{\rho(0)}\approx-\frac{e^{-\Gamma(0)t}}{\Gamma(0)}\sqrt{\frac{2\Gamma_1}{\pi t}}.$$

The population in all the Bloch states with $p\neq 0$ decreases asymptotically towards their steady-state value.

As a reasonable measure for the coherence length we define the quantity

$$\Lambda(t)=\sum_m |mR_m(t)|. \tag{5.11}$$

Its Laplace transform

$$\hat{\Lambda}(\nu)=\frac{1}{\nu}\frac{1}{\cosh\beta(\nu)-1}$$

follows directly after using Eq. (5.7). Laplace inversion gives the simple expression

$$\Lambda(t)=\frac{\Gamma_1}{\Gamma(0)}(1-e^{-\Gamma(0)t}), \tag{5.12}$$

which demonstrates that the time-dependent coherence length increases exponentially to its steady-state value $\Gamma_1/\Gamma(0)$. We notice that the variation of the rate $\Gamma(p)$ of the optical pumping with the quasimomentum is essential for the creation of both a nonuniform momentum distribution and a finite coherence length. The finite steady-state value may be viewed as resulting from the balance between an unbound increase during a jump-free period (see Sec. V D) and the localizing effect of quantum jumps.

C. Dark state and Lévy statistics

The periodic potential $V(x)$ does not have to arise from a position-dependent light shift. As demonstrated by Dum and Ol'shanii [20], even for a dark internal state at all positions a gauge potential arises due to nonadiabatic effects. The ground state in this gauge potential does not decay at all, which gives rise to velocity-dependent coherent population trapping [31].

In the expressions so far it has been tacitly assumed that the decay rate $\Gamma(p)$ is positive for all values of the Bloch parameter p. Now we consider the situation that the atom in the lattice has a nondecaying ground state at $p=0$, which is the case when $\Gamma_0=\Gamma_1$. In the presence of a dark state, one might expect that the overlap of the initial state with the dark

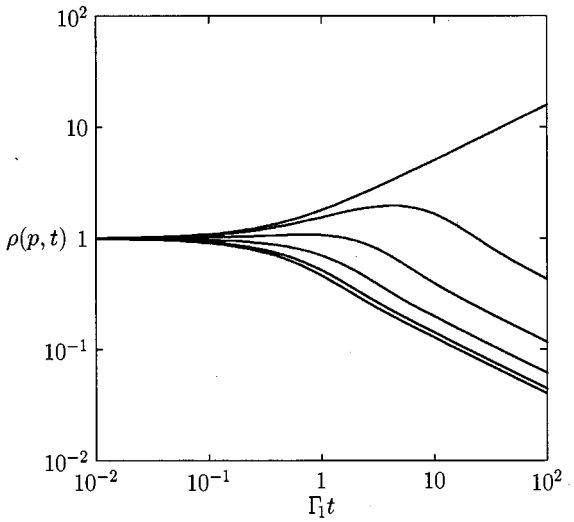

FIG. 4. Time-dependent behavior of $\rho(p,t)$ in the presence of a dark ground state. The values of p are the same as in Fig. 2.

state gives a nonzero probability $p_0(\infty)$ that no jump occurs at any time [28]. In the present case, however, the dark state corresponds to a single p value in a continuum and $p_0(\infty) = 0$. As follows from Eq. (5.5) in the limit $\nu \searrow 0$, this means that the total number of jumps $\hat{f}(0)$ is infinite. The waiting-time distribution w is normalized to one, but it decays so slowly that the average waiting time for the next jump becomes infinite, which implies that the time-averaged jump rate f is zero [28]. Then the jump statistics is described by a Lévy distribution [13].

The Lévy statistics does not give rise to a stationary distribution over the quasimomentum. For $p \neq 0$, the time-dependent distribution is given by the integral expression (5.9). Since $\Gamma(0) = 0$ for the ground state, the zero-jump momentum distribution (5.3) is unity for $p = 0$ and we obtain with Eq. (5.4)

$$\rho(0,t) = 1 + \int_0^t dt' f(t'),$$

which grows monotonically and indefinitely. The long-time behavior is found by applying Eq. (A5) in the Appendix, which gives for the jump rate

$$f(t) \approx \sqrt{\frac{2\Gamma_1}{\pi t}},$$

and for the quasimomentum distribution

$$\rho(p,t) \approx \frac{f(t)}{\Gamma(p)} \quad \text{if} \quad p \neq 0, \quad \rho(0,t) \approx \sqrt{\frac{8\Gamma_1 t}{\pi}}.$$

This distribution is plotted in Fig. 4. The distinctly different asymptote for $p = 0$ shows up most prominently on the double logarithmic scale. The width of the distribution decreases to zero for $t \to \infty$. The coherence length (5.11) now increases linearly in time, according to

$$\Lambda(t) = \Gamma_1 t.$$

In the localization picture of quantum trajectories, each quantum jump puts the atom in a Wannier state, which has a uniform distribution over the quasimomentum p. Hence a quantum jump corresponds to a complete reset of the system. The duration of the jump-free time intervals is governed by the single waiting-time distribution $w(t)$ and the behavior of the quasimomentum distribution is the same during each interval. Nevertheless, the ensemble-averaged quasimomentum density near $p = 0$ increases with time t. This can be explained by noticing that the probability that the last jump took place a long time ago increases with time t. This favors small values of the quasimomentum. In the recoil picture of the trajectories the perspective is dramatically different. Then the quasimomentum has a constant well-defined value during each jump-free period, which suffers a random change at a quantum jump. Atoms accumulate near the dark state simply because there the jump rate is vanishingly low.

D. Conditional distributions

The quantities calculated in the previous subsections were averaged over the full ensemble of trajectories, which corresponds to the solution of the master equation (3.2). It is illuminating to compare these results to the evolution corresponding to the conditional density operator $\boldsymbol{\rho}'(t)$, defined in Eq. (4.3), which refers only to the subensemble of trajectories with no photon emission in the time $[0,t]$. These intervals can be selected in principle by a continuous observation of the atom with photon detectors [32]. The uniform component Γ_0 of the emission rate affects the zero-jump density operator $\boldsymbol{\rho}_0$ only as an overall factor, so that the conditional density operator $\boldsymbol{\rho}'$ does not depend on Γ_0. The conditional jump rate $f'(t)$ has already been given in Eq. (4.8). The conditional coherence functions $R'_m(t)$ are defined as in Eq. (5.2), with $\boldsymbol{\rho}'$ replacing $\boldsymbol{\rho}$. From the Fourier expansion (A2) of $\rho_0(p)$ and the normalization constant (4.6) we obtain

$$R'_m(t) = \frac{I_m(\Gamma_1 t)}{I_0(\Gamma_1 t)}.$$

Notice that $R'_m(t)$ is positive definite.

The corresponding conditional coherence length $\Lambda'(t)$ as defined in analogy to Eq. (5.11) can be calculated after noticing that Eq. (A3) gives the Laplace transform of $p_0(t)R'_m(t)$, while Eq. (A4) is the Laplace transform of $R_m(t)$. By comparison of their right-hand sides, one notices that

$$t\frac{d}{dt}R_m(t) = |m| p_0(t) R'_m(t),$$

which gives, after summation, the expression for the conditional coherence length

$$\Lambda'(t) = \frac{t}{p_0(t)} \frac{d}{dt}\rho(0,t)$$

in terms of the quasimomentum distribution at $p = 0$. Use of Eq. (5.9) then gives

$$\Lambda'(t)=\frac{\Gamma_1 t}{I_0(\Gamma_1 t)}\left[e^{\Gamma_1 t}-\int_0^t dt'\,\frac{e^{\Gamma_1(t-t')}}{t'}I_1(\Gamma_1 t')\right].$$

This conditional coherence length increases indefinitely, in contrast to its average counterpart (5.12). Therefore, in order to obtain atomic states with a large coherence length, it can be advantageous to wait for a long dark time interval rather than taking an arbitrary moment in time. Long dark periods are rare, except in the presence of a dark state.

VI. SPATIAL DISTRIBUTIONS AND DIFFUSION

A. Photon and atom distributions

An atom that is initially localized in a Wannier state will get delocalized due to a combination of coherent tunneling through the barriers and incoherent diffusion due to photon emission. This spreading of the atomic state shows up in the time dependence of the populations of the Wannier states

$$\rho_n(t)=\langle\phi_n|\boldsymbol{\rho}(t)|\phi_n\rangle.$$

Alternatively, the atomic delocalization reveals itself in the spatial distribution of the emitted photons

$$P_n(t)=\frac{f_n(t)}{f(t)},$$

which differs from ρ_n unless the decay rate $\Gamma(p)$ is uniform.

From the master equation (3.2) it follows that the partial detection rates (3.8) are related to the partial waiting-time distributions (4.7) by

$$f_n(t)=w_n(t)+\sum_{n'}\int_0^t dt'\,w_{n-n'}(t-t')f_{n'}(t').$$

The generating functions

$$F(q,t)=\sum_n e^{2\pi i n q}f_n(t),\quad W(q,t)=\sum_n e^{2\pi i n q}w_n(t)$$

are connected through their Laplace transforms as

$$1+\hat{F}(q,\nu)=\frac{1}{1-\hat{W}(q,\nu)}.$$

The spreading of the state of an atom can be characterized by the spatial width $\Delta(t)$, defined by

$$\Delta^2(t)=\sum_n n^2 P_n(t).$$

The diffusion constant D, defined by [33]

$$\Delta^2(t)\approx Dt\quad\text{for}\quad t\to\infty,$$

can be calculated from

$$D=\lim_{\nu\searrow 0}\frac{-\nu^2}{4\pi^2\overline{f}}\frac{d^2\hat{F}}{dq^2}(0,\nu)=\frac{-\overline{f}}{4\pi^2}\frac{d^2\hat{W}}{dq^2}(0,0).\qquad(6.1)$$

From the explicit expression (4.7) one derives

$$\frac{-1}{4\pi^2}\frac{d^2\hat{W}}{dq^2}(0,\nu)=2\tan^2\alpha[(\Gamma_0+\nu)\hat{p}_0(\nu)-1]+\hat{f}(\nu)-\frac{\overline{f}}{\nu}-4A^2\left[(\Gamma_0+\nu)\hat{p}_0^3(\nu)-\frac{\Gamma_0}{\overline{f^3}}\right],$$

with the complex parameter $Ae^{i\alpha}=iE+\frac{1}{2}\Gamma_1$. Inversion to the time domain gives an expression containing integrals over the jump rate $f(t)$ and over $p_0(t)$. The diffusion constant (6.1) is

$$D=(2\tan^2\alpha+1)(\Gamma_0-\overline{f})=\frac{8E^2+\Gamma_1^2}{\Gamma_0+\overline{f}}.$$

The dependence of D on both tunneling rates E and Γ_1 is monotonically increasing, so that diffusion is maximal when a dark state is present. The dependence on the uniform component Γ_0 is inverse, showing that a large overall decay rate hampers the spatial diffusion. This may be understood as arising from the localizing effect of spontaneous emission. In fact, since spontaneous emission may be regarded as a position measurement of the atom, the reduction of spatial diffusion by large values of Γ_0 is analogous to the quantum Zeno effect.

B. Uniform decay rate

In the special case of a uniform decay rate $\Gamma(p)=\Gamma_0$ the partial waiting-time distribution is explicitly

$$w_n(t)=\Gamma_0 e^{-\Gamma_0 t}J_n^2(Et),$$

which has the Laplace transformed generating function

$$\hat{W}(q,\nu)=\frac{\Gamma_0}{\sqrt{(\nu+\Gamma_0)^2+(2E\,\sin\pi q)^2}}.$$

The time-dependent width obeys the simple expression

$$\Delta^2(t)=Dt+\frac{D}{\Gamma_0}(e^{-\Gamma_0 t}-1)$$

in terms of the diffusion coefficient $D=4E^2/\Gamma_0$.

C. Conditional spatial distributions

The conditional population in well n is obtained from the pure state (4.3) with Eq. (A2) in terms of Bessel functions with a complex argument

$$\rho_n'(t)=\frac{1}{I_0(\Gamma_1 t)}|I_n(Ate^{i\alpha})|^2.$$

It describes how far an atom can travel between two jumps. The width of the atomic wave function a time t after the last photon detection is found as

$$At\sqrt{\frac{R_1'(t)}{\Gamma_1 t}}.$$

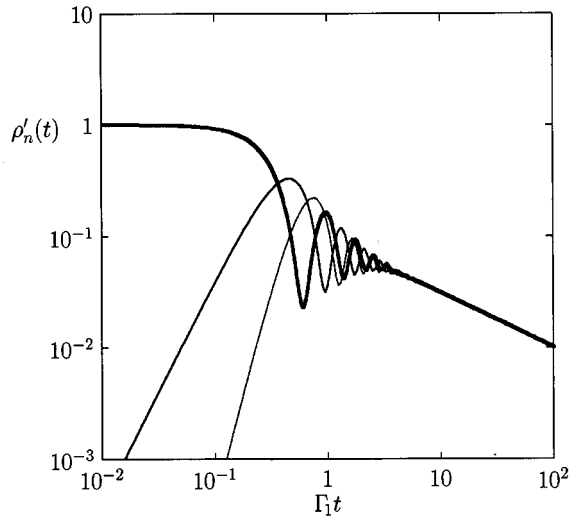

FIG. 5. Conditional Wannier populations $\rho'_n(t)$ in well $n=0$, and 1, and 2 as a function of time. The coherent tunneling rate is $E=4\Gamma_1$.

In contrast to the coherence length Λ', this width depends not only on Γ_1 but also on the coherent tunneling rate E. The width of both the coherent and the incoherent atomic distributions ρ'_n and ρ_n initially increases linearly.

The conditional distribution

$$P'_n(t)=\frac{f'_n(t)}{f'(t)}=\frac{w_n(t)}{w(t)}$$

describes the probability distribution of the detected photon over the locations n. Hence P'_n give the probability that the pure state $|\psi(t)\rangle$ is reduced to the Wannier state $|\phi_n\rangle$ by a localized photon detection. With Eq. (4.7) the corresponding width can be evaluated, with the result

$$\Delta'^2(t)=\Gamma_1\frac{\overline{R_1}-R_1(t)}{4w(t)}+\frac{A^2t}{\Gamma_1}\frac{\Gamma_0R'_1(t)-\Gamma_1}{f'(t)}+\frac{2E^2}{\Gamma_1}\frac{R'_1(t)}{f'(t)}.$$

Note that the initial value is $(\Gamma_0-\overline{f})/4\Gamma_0$, so that rapid photon emissions can force the atom to move fast to a different well.

In the case of a uniform decay rate, the distributions of both the atom and the first detected photon

$$\rho'_n(t)=P'_n(t)=J_n^2(Et)$$

equal the Wannier populations in the solution (2.9) for pure Hamilton evolution. A nonuniform decay rate strongly damps the oscillatory behavior of ρ'_n and P'_n, so that also the conditional distributions behave diffusively on long time scales. This can be seen in Fig. 5.

VII. CONCLUSION

We analyze the quantum-mechanical transport properties of atoms in an optical lattice. The atomic dynamics may be viewed as resulting from the balance between Hamiltonian evolution, which gives a spreading of the wave packet over many lattice sites, and optical pumping, which tends to localize the atom. The atoms are assumed to be tightly bound in a single Bloch band in a single adiabatic potential. Then the internal state of the atoms is fully eliminated and the system is parametrized in terms of just a few relevant quantities. Key quantities are the energy bandwidth $2E$ and the variation of the optical-pumping rate over the band. The transport behavior of the atom is governed by a master equation for the density operator and the evolution is conveniently represented as an ensemble of pure-state quantum trajectories, where the coherent evolution of the wave function is randomly interrupted by quantum jumps. Individual trajectories depend strongly on whether the jumps correspond to the detection of a photon with a well-defined momentum or at a well-defined location. The first case leads to the recoil picture, where the atom is in a Bloch state at all times and jumps simply transfer the atom from one Bloch state to another one. In the second case, a quantum jump localizes the atom in a single potential well, which in the tight-binding limit corresponds to a Wannier state. In between jumps, the atom can tunnel through the barriers from one well to the next one. In the steady state, the density operator is diagonal in the Bloch states, so that it is translationally invariant. The coherence length, which indicates the degree of quantum localization, remains finite. We derive analytical expressions for the jump statistics, such as the time-dependent jump rate and the waiting-time distribution. The coherence length as a function of time is expressed in terms of the quasimomentum distribution. Also the net diffusion coefficient for the spreading of the atom over the lattice can be expressed analytically. The spatial distributions of the atoms and of the emitted photons are related, but not identical. The special case of a dark state is modeled by setting the jump rate equal to zero at zero quasimomentum. This describes the situation of coherent population trapping that is selective in the quasimomentum. The average waiting time is infinite, even though the waiting-time distribution is normalized to one, and each jump is followed by a next one in the long run. The jump statistics, which is governed by Lévy statistics, can still be treated analytically.

ACKNOWLEDGMENTS

This work is part of the research program of the Foundation for Fundamental Research on Matter (FOM) and was made possible by financial support from the Netherlands Organization for Scientific Research (NWO).

APPENDIX: LAPLACE TRANSFORMS

Laplace transforms are denoted as in

$$\hat{f}(\nu)=\int_0^\infty dt e^{-\nu t}f(t).$$

We summarize a few identities that allow us to evaluate Laplace inversions occurring in the text. We consider the Fourier series

$$\frac{\sinh\beta}{\cosh\beta-\cos2\pi p}=\sum_m e^{-|m|\beta}e^{2\pi imp}, \qquad \text{(A1)}$$

which follows from direct summation. We expand $\rho_0(p,t)$ in modified Bessel functions as

$$e^{-\Gamma_0 t+\Gamma_1 t\,\cos 2\pi p}=\sum_m e^{-\Gamma_0 t}I_m(\Gamma_1 t)e^{2\pi imp}, \qquad \text{(A2)}$$

while noticing that the Laplace transform of this equation has the same p dependence as Eq. (A1). A comparison of these two summation leads to the identity

$$\frac{e^{-|m|\beta(\nu)}}{\Gamma_1\sinh\beta(\nu)}=\int_0^\infty dt e^{-\nu t}e^{-\Gamma_0 t}I_m(\Gamma_1 t), \qquad \text{(A3)}$$

where ν and β are related by the identity $\cosh\beta(\nu)=(\nu+\Gamma_0)/\Gamma_1$. Equation (A3) determines the Laplace inversion of its left-hand side in terms of a modified Bessel function. One easily checks that Eq. (A3) is simply proportional to the derivative of $\exp(-|m|\beta)$ with respect to ν, since $d\beta/d\nu=1/(\Gamma_1\sinh\beta)$. Recall that differentiating a Laplace transform with respect to ν is equivalent to multiplying the original time-dependent function by $-t$. Conversely, differentiating a time-dependent function is equivalent to multiplying its Laplace transform with ν, provided that the function disappears at $t=0$. This way one can prove from Eq. (A3) that for $m\neq 0$,

$$\frac{e^{-|m|\beta(\nu)}}{\nu}=|m|\int_0^\infty dt e^{-\nu t}\int_0^t dt'\,\frac{e^{-\Gamma_0 t'}}{t'}I_m(\Gamma_1 t'). \qquad \text{(A4)}$$

The asymptotic behavior for large times follows from the behavior of the Laplace transform around $\nu=0$. One checks that if and only if

$$f(t)\approx\frac{se^{-\gamma t}}{\sqrt{\pi t}}\left[\frac{1}{t^n}+O\left(\frac{1}{t^{n+1}}\right)+\cdots\right] \quad \text{for} \quad t\to\infty,$$

where $s\neq 0$, then

$$\lim_{\nu\searrow 0}\sqrt{\nu}\left(\frac{-d}{d\nu}\right)^n\hat{f}(\nu-\gamma)=s. \qquad \text{(A5)}$$

In the special case $\gamma=0$, $n=0$, this is easily demonstrated by using that $1/\sqrt{\nu}$ is the Laplace transform of $1/\sqrt{\pi t}$. The extension to positive values of γ and n follows with standard Laplace rules.

[1] N. P. Bigelow and M. G. Prentiss, Phys. Rev. Lett. **65**, 29 (1990).
[2] P. Verkerk, B. Lounis, C. Salomon, C. Cohen-Tannoudji, J.-Y. Courtois, and G. Grynberg, Phys. Rev. Lett. **68**, 3861 (1992).
[3] P. Jessen, C. Gerz, P. D. Lett, W. D. Phillips, S. L. Rolston, R. J. C. Spreeuw, and C. I. Westbrook, Phys. Rev. Lett. **69**, 49 (1992).
[4] A. Hemmerich and T. W. Hänsch, Phys. Rev. Lett. **70**, 410 (1993).
[5] G. Grynberg and J.-Y. Courtois, Europhys. Lett. **27**, 41 (1994).
[6] P. S. Jessen and I. H. Deutsch, Adv. At. Mol. Opt. Phys. **37**, 95 (1996).
[7] B. P. Anderson, T. L. Gustavson, and M. A. Kasevich, Phys. Rev. A **53**, R3727 (1996).
[8] C. Jurczak, B. Desruelle, K. Sengstock, J.-Y. Courtois, C. I. Westbrook, and A. Aspect, Phys. Rev. Lett. **77**, 1727 (1996).
[9] M. B. Dahan, E. Peik, J. Reichel, Y. Castin, and C. Salomon, Phys. Rev. Lett. **76**, 4508 (1996).
[10] Q. Niu, X.-G. Zhao, G. A. Georgakis, and M. G. Raizen, Phys. Rev. Lett. **76**, 4504 (1996).
[11] S. R. Wilkinson, C. F. Bharucha, K. W. Madison, Q. Niu, and M. G. Raizen, Phys. Rev. Lett. **76**, 4512 (1996).
[12] S. Marksteiner, K. Ellinger, and P. Zoller, Phys. Rev. A **53**, 3409 (1996).
[13] F. Bardou, J. P. Bouchaud, O. Emile, A. Aspect, and C. Cohen-Tannoudji, Phys. Rev. Lett. **72**, 203 (1994).
[14] N. W. Ashcroft and N. D. Mermin, *Solid State Physics* (Saunders, Philadelphia, 1976).
[15] T. Müller-Seydlitz, M. Hartl, B. Brezger, H. Hänsel, C. Keller, A. Schnetz, R. J. C. Spreeuw, T. Pfau, and J. Mlynek, Phys. Rev. Lett. **78**, 1038 (1997).
[16] T. Esslinger, F. Sander, A. Hemmerich, and T. W. Hänsch, Opt. Lett. **21**, 991 (1996).
[17] H. Stecher, H. Ritsch, P. Zoller, F. Sander, T. Esslinger, and T. W. Hänsch, Phys. Rev. A **55**, 545 (1997).
[18] P. L. Haycock, S. E. Hamann, G. Klose, and P. S. Jessen, Phys. Rev. A **55**, R3991 (1997).
[19] P. L. Gould, G. A. Ruff, and D. E. Pritchard, Phys. Rev. Lett. **56**, 827 (1986).
[20] R. Dum and M. Ol'shanii, Phys. Rev. Lett. **76**, 1788 (1996).
[21] G. Lindblad, Commun. Math. Phys. **48**, 119 (1976).
[22] J. Dalibard, Y. Castin, and K. Mølmer, Phys. Rev. Lett. **68**, 580 (1992).
[23] C. W. Gardiner, A. S. Parkins, and P. Zoller, Phys. Rev. A **46**, 4363 (1992).
[24] H. J. Carmichael, *An Open System Approach to Quantum Optics* (Springer, Berlin, 1993).
[25] M. Holland, S. Marksteiner, P. Marte, and P. Zoller, Phys. Rev. Lett. **76**, 3683 (1996).
[26] G. Nienhuis, J. de Kloe, and P. van der Straten, J. Opt. Soc. Am. B **12**, 520 (1995).
[27] R. Dum, P. Zoller, and H. Ritsch, Phys. Rev. A **45**, 4879 (1992).
[28] P. M. Visser and G. Nienhuis, Phys. Rev. A **52**, 4727 (1995).
[29] S. Reynaud, Ann. Phys. (Paris) **8**, 315 (1983).
[30] G. Nienhuis, J. Stat. Phys. **53**, 417 (1988).
[31] A. Aspect, E. Arimondo, R. Kaiser, N. Vansteenkiste, and C. Cohen-Tannoudji, Phys. Rev. Lett. **61**, 826 (1988).
[32] D. Bouwmeester and G. Nienhuis, Quantum Semiclassic. Opt. **8**, 277 (1996).
[33] N. G. van Kampen, *Stochastic Processes in Physics and Chemistry* (North-Holland, Amsterdam, 1981).